Soils and Rocks

An International Journal of Geotechnical and Geoenvironmental Engineering

www.soilsandrocks.com

ISSN 1980-9743
ISSN-e 2675-5475

Comparative study of deterministic and probabilistic critical slip surfaces applied to slope stability using limit equilibrium methods and the First-Order Reliability Method

Higor Biondo de Assis[1#], Caio Gorla Nogueira[1]

Article

Keywords
Slope stability
Limit equilibrium methods
Factor of safety
Direct coupling
Reliability
Quantitative risk assessment

Abstract

This work presents the validation of the Morgenstern-Price method implemented in the Risk Assessment applied to Slope Stability (RASS) computational program to carry out deterministic and probabilistic analyses of slope stability. Deterministic analyses, based on the factor of safety approach, are performed using limit equilibrium methods. The probabilistic ones, on the other hand, are carried out through the direct coupling of these methods to the First Order Reliability Method (FORM). Initially, two benchmark cases are presented for validation of the computational routine related to the Morgenstern-Price method. Next, two illustrative examples are presented, with the investigation of the critical surfaces defined by deterministic and probabilistic criteria, which correspond to the minimum factor of safety, the maximum probability of failure, and the maximum quantitative risk. In the set of stability analyses, it was verified that both the numerical responses and the geometry of the critical surfaces can vary depending on the choice of the limit equilibrium method and the criterion for identifying the critical surface. The different possibilities presented by the methodology used in this study define not only a critical surface, but a set of critical surfaces that can help in the engineering decision-making process and slope risk management, complementing the widely used purely deterministic analyses in geotechnics.

1. Introduction

The problem of slope stability is quite recurrent in everyday life, whether on natural or built slopes. Every year several cases of failure are reported in the most diverse places around the world, especially in inhabited places, on highways, railways or even in the mining industry. The causes can be diverse, either by anthropic actions, extreme natural phenomena or a combination of both. For this reason, geotechnical engineering is also dedicated to the study of this type of engineering problem, in which the consequences usually cause economic and environmental damage and loss of human lives, for instance.

In traditional deterministic analyses of slope stability, the uncertainties related to the problem are commonly neglected. The better understanding of these uncertainties, intrinsic or epistemic, has become an object of great interest in geotechnical research in the last two decades (Jiang et al., 2022).

The intrinsic uncertainties are mainly related to the spatial variability of the materials that constitute the analyzed engineering systems. In slope stability problems, the natural variability of soil strength and other properties is a source of intrinsic uncertainty. On the other hand, the epistemic uncertainties, those that theoretically can be reduced by the adoption of good practices, are originated by diverse sources, such as simplified mathematical mechanical models, ground investigation methods, as well as the difficulty to reproduce in laboratory what happens in nature (Melchers & Beck, 2018). All these practices allow simplifications in order to make it possible for Geotechnical Engineering to perform consistent analyses, although they are not exact (Husein Malkawi et al., 2000).

An important source of epistemic uncertainty in slope stability analysis is the variability of the answers provided by the limit equilibrium methods widely used in most of the software dedicated to this discipline. In this context, the aim of this paper is to show how deterministic and probabilistic responses behave as a function of the choice of different limit equilibrium methods. The deterministic analyses are performed from the factor of safety (*FS*) concept, and the probabilistic analyses, from the direct coupling of these limit equilibrium

[#]Corresponding author. E-mail address: higor.assis@unesp.br
[1]Universidade Estadual Paulista, Departamento de Engenharia Civil e Ambiental, Bauru, SP, Brasil.

Submitted on December 3, 2022; Final Acceptance on April 1, 2023; Discussion open until August 31, 2023.
https://doi.org/10.28927/SR.2023.013522

methods to the First-Order Reliability Method (Ang & Tang, 1984). The variability of *FS* considering several limit equilibrium methods is discussed when the analyses are performed by deterministic and especially probabilistic approaches.

2. Methodology

Probabilistic analyses of slope stability can be performed using different methodologies such as direct coupling of limit equilibrium methods to reliability methods and simulation techniques (Leonel et al., 2011; Siacara et al., 2020). In this approach, the transformation methods are used to provide the probabilistic response for each of the listed failure modes. Each failure mode is represented by a limit state function, which is a response given by a representative mechanical model (Phoon, 2008). In the slope stability problem, the *FS* is the response provided by the limit equilibrium methods, which feeds the probabilistic model and represents the failure mode, which is the rupture of the slope by shear. To carry out the analyses presented in this paper, it was used the program Risk Assessment applied to Slope Stability (RASS), developed by the authors for deterministic and probabilistic analyses of slope stability. The Morgenstern-Price method implemented in RASS follows the formulation presented in detail by Zhu et al. (2005). RASS also has the Ordinary, Simplified Bishop (Bishop) (Bishop, 1955), Simplified Janbu (Janbu) and Corrected Simplified Janbu (Janbu (f_0)) methods (Janbu, 1954a, b, 1973). The Spencer method (Spencer, 1967, 1973) is a particular case of the Morgenstern-Price method (Morgenstern & Price, 1965), contemplated by the formulation presented in this paper. The detailed formulation of the mentioned limit equilibrium methods are presented by Fredlund & Krahn (1977), Abramson et al. (2001).

2.1 Morgenstern-Price method

Several limit equilibrium methods, based on the slice method, have been developed throughout the 20th century for slope stability analyses. These methods are based on statics equations and require some assumptions to make the problem statically determined. In general, these assumptions are related to the interslice normal forces and interslice tangential forces. The Morgenstern-Price method is considered a rigorous method because it completely satisfies the equilibrium of forces in two directions and moments (Morgenstern & Price, 1965). To make this possible, the method adopts an interslice force function, which relates the tangential forces to the normal forces acting on the sides of the slices positioned on the abscissa *x*, establishing a relationship that can be constant or variable along the horizontal extension of the slope slip surface, according to Equation 1:

$$S = \lambda \bullet f\left(x\right) \bullet E \tag{1}$$

where *S* is the tangential interslice force, *E* is the normal interslice force, λ is an unknown scaling factor e *f(x)* is the interslice force function. As presented by Zhu et al. (2005), *f(x)* can be written as given by Equation 2:

$$f\left(x\right) = sen^{\mu}\left[\pi\left(\frac{x - x_L}{x_R - x_L}\right)^{\nu}\right] \tag{2}$$

where x_L and x_R are abscissa of the left and right ends of the failure surface, respectively, so that $x \in \left[x_L, x_R\right]$. Therefore, the *FS* can be written as presented by Equation 3:

$$FS = \frac{\sum_{i=1}^{n-1}\left(R_i \prod_{j=i}^{n-1}\psi_j\right) + R_n}{\sum_{i=1}^{n-1}\left(T_i \prod_{j=i}^{n-1}\psi_j\right) + T_n} \tag{3}$$

in which, R_i is the sum of the shear resistances contributed by all forces acting on the *i*th slice except the normal shear forces, and T_i is the sum of the components of these forces tending to cause instability, as given by Equations 4 and 5:

$$\begin{aligned} R_i = &\left[W_i \cos\alpha_i + Q_i \cos\left(\omega_i - \alpha_i\right) - U_i\right] \bullet \\ &\tan\varphi_i' + c_i' b_i \sec\alpha_i \end{aligned} \tag{4}$$

$$T_i = W_i sen\alpha_i - Q_i sen\left(\omega_i - \alpha_i\right) \tag{5}$$

where W_i is the self-weight of *i*th slice, a_i is the slope of the base of the slice relative to the horizontal, Q_i is the external force acting on the *i*th slice, w_i is the angle between the vertical and the direction of the external force Q_i, U_i is the resultant water force acting on the base of the *i*th slice, φ_i' is the soil friction angle along the base of the *i*th slice, c_i' is the soil cohesion along the base of the *i*th slice. From imposing the force equilibrium of *i*th slice and resolving in the perpendicular direction and in the direction parallel to the slip surface, and substituting the former into the latter, Equation 6 is given in the form:

$$\begin{aligned} &E_i\left[\left(\sin\alpha_i - \lambda f_i cos\alpha_i\right)tan\varphi_{i'} + \left(cos\alpha_i + \lambda f_i sin\alpha_i\right)FS\right] = \\ &E_{i-1}\left[\left(sin\alpha_i - \lambda f_{i-1} cos\alpha_i\right)tan\varphi_{i'} + \left(cos\alpha_i + \lambda f_{i-1} sin\alpha_i\right)FS\right] + \\ &FST_i - R_i \end{aligned} \tag{6}$$

where E_i and E_{i-1} corresponds to the normal interslice forces acting on the left and right side of *i*th slice, respectively, and f_i and f_{i-1} are the values of f(x) assumed on the left and right side of the *i*th slice, respectively.

Equations 7, 8 and 9 refer to a rearrangement of the equations using the variables ψ_{i-1}, ϕ_{i-}, ϕ_i for changing variables:

$$\psi_{i-1} = \begin{bmatrix} \left(sen\alpha_i - \lambda f_{i-1} \cos\alpha_i\right)\tan\varphi_i' + \\ \left(\cos\alpha_i + \lambda f_{i-1} sen\alpha_i\right)FS \end{bmatrix} / \phi_{i-1} \tag{7}$$

$$\phi_{i-1} = \left(sen\alpha_{i-1} - \lambda f_{i-1}\cos\alpha_{i-1}\right)\tan\varphi_{i-1}' + \left(\cos\alpha_{i-1} + \lambda f_{i-1} sen\alpha_{i-1}\right)FS \tag{8}$$

$$\phi_{i} = \left(sen\alpha_{i} - \lambda f_{i}\cos\alpha_{i}\right)\tan\varphi_{i}' + \left(\cos\alpha_{i} + \lambda f_{i} sen\alpha_{i}\right)FS \tag{9}$$

According to the Morgenstern-Price method, the value of FS is defined at the intersection between the curves of the factor of safety of forces (FS_f) and the factor of safety of moments (FS_m) as a function of λ. The calculation of λ is given according to the Equation 10:

$$\lambda = \frac{\sum_{i=1}^{n}\left[b_i\left(E_i + E_{i-1}\right)\tan\alpha_i + 2Q_i sen\omega_i h_i\right]}{\sum_{i=1}^{n}\left[b_i\left(f_i E_i + f_{i-1}E_{i-1}\right)\right]} \tag{10}$$

2.2 First-Order Reliability Method

The First-Order Reliability Method (FORM) has been widely used in structural reliability (Ang & Tang, 1984). Recently, FORM has been also considered as an important alternative to Monte Carlo Simulation method (MCS) (Cho, 2007, 2010) in probabilistic slope stability analysis, since it provides significantly lower computational cost (Ji et al., 2018; Siacara et al., 2022). The method involves defining a representative failure mode function, which is linearised from the Taylor series expansion by a tangent hyperplane around the most probable failure point, named the design point (***y****). This function is called the limit state function (*g(**X**)*), in which ***X*** is a vector of random variables associated with the problem ($\boldsymbol{X} = \left[X1, X2, \ldots, Xn\right]^T$). In summary, it consists in solving an optimization problem, which seeks to find ***y****, in order to minimizes the reliability index (β), subject to $g\left(\boldsymbol{X}\right) = 0$. The solution of the problem is performed using the Hasofer-Lind-Rackwitz-Fiessler (HLRF) algorithm (Hasofer & Lind, 1974; Rackwitz & Fiessler, 1978), and requires the transformation of the random variables from the physical space ($\mathbb{X}$) to the standard uncorrelated normal space ($\mathbb{Y}$) (Lebrun & Dutfoy, 2009), where β is defined, according to Equation 11:

$$\beta = \sqrt{(\boldsymbol{y}^*)^T\left(\boldsymbol{y}^*\right)} \tag{11}$$

Thus, the probability of failure, given by $Pf = P\left[g\left(\boldsymbol{X}\right) \le 0\right]$ can be estimated as Equation 12:

$$Pf \approx \Phi\left(-\beta\right) \tag{12}$$

in which $\Phi\left(\bullet\right)$ is the standard normal cumulative distribution function (Ang & Tang, 1984).

2.3 Slope stability limit state function

Slope stability analyses consist of assessing the shear strength of the soil mass on a given slip surface. According to the limit equilibrium theory, the slope instability is verified when FS ≤ 1. In agreement with this condition, the limit state function is given by Equation 13:

$$g\left(\boldsymbol{X}\right) = FS\left(\boldsymbol{X}\right) - 1.00 \tag{13}$$

Thus, the solution of the slope stability problem, according to the reliability approach, provides a probabilistic response that represents the probability of the *FS* of the slope assuming a value less than or equal to 1.00 (Fenton & Griffiths, 2008).

2.4 Quantitative risk assessment

One of the widely accepted definitions of risk is that it can be quantified from the product of the probability of failure and the consequence associated with that failure (Melchers & Beck, 2018). In the probabilistic stability analyses of two-dimensional slopes, the values of *Pf* are obtained for the evaluated multiple surfaces of rupture. Each of these surfaces has a mobilized soil area corresponding to the sum of the areas of the lamellae. This area is also called the active zone and is delimited by the slope surface and the slip surface. Considering a slope strip of unit width, the consequence of shear failure can be represented in a simplified way by the constant *C* (Jiang et al., 2022; Zhang & Huang, 2016), which represents the mobilized volume of soil ($\left[C\right] = L^3L^{-1}$). Thus, for the slope stability problem, the quantitative risk (*Rv*) can be written according to Equation 14:

$$Rv = P_f \bullet C \tag{14}$$

2.5 Criteria for identifying critical slip surfaces

According to the deterministic approach to slope stability, the critical slip surface is defined by investigation and identified from the lowest calculated *FS* value, among a predefined set of trial slip surfaces. In this way, the minimum *FS* value (FS_{min}) is the criterion that defines the critical deterministic slip surface. Conversely, the critical probabilistic slip surfaces can be defined by different criteria, such as maximum *Pf* value (Pf_{max}) and maximum *Rv* (Rv_{max}) value, according to the methodology presented for carrying out the probabilistic analyses via direct coupling of the limit equilibrium methods to the FORM.

2.6 Benchmarks

Two cases are presented to validate the RASS code implemented to evaluate the *FS* using the Morgenstern-Price method. In both cases the slopes consist of homogeneous soil and the same slip surface is evaluated. The difference is that in case 2 there is the inclusion of the piezometric line, while in case 1 there is not, as presented in Figure 1:

The Morgenstern-Price formulation implemented in RASS followed the algorithm presented by Zhu et al. (2005)

and for this reason these cases were chosen for validation of the computational code written by the authors. The geotechnical parameters used in the analyses are the same as in the original example. For deterministic analyses, only the mean values (μ_X) of the random variables are used. Table 1 brings a description of the variability of these parameters, with their respective coefficients of variation (COV_X) and probability density function (PDF_X) that best describes the random variable X:

The values of COV_X and PDF_X will be used only in the probabilistic analyses, at the appropriate moment of this work. It is important to note that Spencer's method is a particular case of the Morgenstern-Price method, where *f(x)* takes constant value over the entire domain of *x*. According to this particularity, Table 2 presents the *FS* and λ values calculated with the RASS program using the Spencer's method, in which interslice force function is constant ($\mu = \nu = 0 \Rightarrow f(x) = 1$):

Table 3 presents the *FS* and λ results for the Morgenstern-Price method with variable *f(x)*, called half-sine function, in which $\mu = \nu = 1$:

As shown, RASS provided results very similar to those reported by the reference papers, with maximum relative errors of 0.109% and 0.309% for *FS* and λ, respectively. These results then allow the validation of the Morgenstern-Price method calculation routine included in RASS, to be used in direct coupling.

Table 1. Variability of geotechnical parameters according to Phoon & Kulhawy (1999).

X	*c'* (kPa)	ϕ' (º)
μ_X	28.74	20.00
COV_X	30%	10%
PDF_X	Lognormal	Lognormal

The soil unit weight (y) was considered as a deterministic variable: *y* = 18.85 kN/m³.

2.7 Critical slip surfaces

As an extension of the benchmarks presented, in this section a set of deterministic and probabilistic analyses is presented, with investigation of the critical surfaces of the slopes relative to cases 1 and 2. About 10,000 experimental

Table 2. Comparison of FS and l values computed by RASS using Spencer's method.

Case	*FS*			λ			*Error* (%)*	
	Fredlund & Krahn (1977)	Zhu et al. (2005)	RASS	Fredlund & Krahn (1977)	Zhu et al. (2005)	RASS	*FS*	λ
1	2.076	2.075	2.074	0.254	0.258	0.258	0.048	0.000
2	1.833	1.831	1.833	0.234	0.240	0.240	0.109	0.000

* Relative error between values reported by Zhu et al. (2005) and RASS.

Table 3. Comparison of *FS* and λ values computed by RASS using Morgenstern-Price method.

Case	*FS*			λ			*Error* (%)*	
	Fredlund & Krahn (1977)	Zhu et al. (2005)	RASS	Fredlund & Krahn (1977)	Zhu et al. (2005)	RASS	*FS*	λ
1	2.076	2.074	2.073	0.318	0.324	0.323	0.096	0.309
2	1.832	1.831	1.832	0.290	0.299	0.299	0.055	0.000

* Relative error between values reported by Zhu et al. (2005) and RASS.

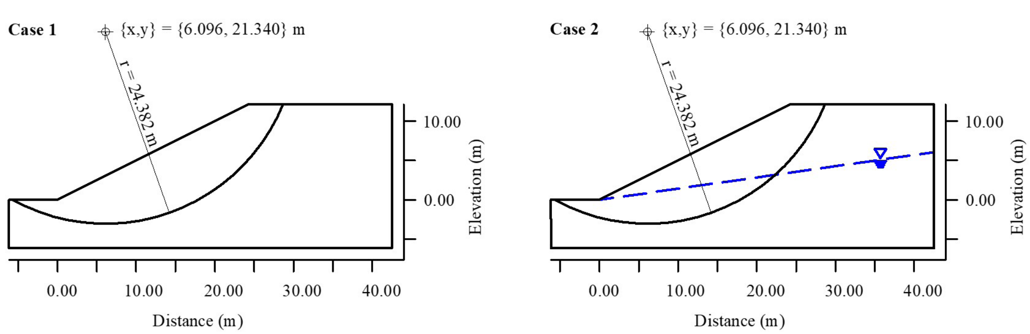

Figure 1. Benchmark cases (Zhu et al., 2005).

sliding surfaces were analysed, using different limit equilibrium methods. The surfaces analysed are circular and defined by the coordinates of centre (x_c, y_c) and radius (r). The critical surfaces were identified according to the deterministic and probabilistic criteria of FS_{min}, Pf_{max} and Rv_{max}. The results are presented in Table 4:

Figure 2 illustrates the deterministic and probabilistic critical surfaces, defined by the different identification criteria and limit equilibrium methods used in the analyses:

The knowledge of the geometry of the critical surface of a slope is important because it is the boundary between the passive and active zones, which corresponds to the volume of soil to be mobilized in an eventual slope rupture. Knowing the boundary that delimits these zones is essential for project development or even the verification of existing reinforced slopes, for example. In a nail-reinforced slope, the length of the anchors that enter the passive zone is determinant in the safety condition of the system. Therefore, if there are uncertainties in the methods employed in the analyses, due to the simplifying hypotheses that they adopt, it is expected that different critical surfaces are identified, as well as different safety levels are observed through the values of FS_{min}, Pf_{max} and Rv_{max}. Another behaviour observed is the position of the Rv_{max} surfaces, which in most cases were positioned between the deeper FS_{min} and shallower Pf_{max} surfaces. This was the main reason for the adoption of the

Table 4. Results of the deterministic and probabilistic critical slip surfaces for cases 1 and 2.

Case	Limit equilibrium method	Criterion	x_c (m)	y_c (m)	R (m)	FS	β	Pf	Rv (m³/m)
1	Bishop	FS_{min}	7.0000	25.0000	25.9608	1.9959	5.2161	9.15E-08	1.39E-05
		Pf_{max}	5.0000	25.7500	26.2336	2.0377	4.9977	2.91E-07	3.35E-05
		Rv_{max}	5.0000	25.7500	26.2336	2.0377	4.9977	2.91E-07	3.35E-05
	Janbu	FS_{min}	8.2500	19.5000	21.6113	1.8333	4.5201	3.09E-06	5.48E-04
		Pf_{max}	6.2500	21.5000	22.7350	1.8725	4.3614	6.47E-06	8.67E-04
		Rv_{max}	6.7500	21.0000	22.4334	1.8544	4.3714	6.18E-06	8.90E-04
	Janbu (f_0)	FS_{min}	8.0000	21.0000	22.7779	1.9860	5.2119	9.36E-08	1.60E-05
		Pf_{max}	5.5000	24.5000	25.2043	2.0374	4.9897	3.03E-07	3.72E-05
		Rv_{max}	5.7500	24.0000	24.8103	2.0284	4.9956	2.94E-07	3.72E-05
	Spencer	FS_{min}	7.0000	25.0000	25.9608	1.9926	5.1999	9.99E-08	1.52E-05
		Pf_{max}	4.7500	26.0000	26.4172	2.0460	4.9748	3.27E-07	3.64E-05
		Rv_{max}	5.0000	25.7500	26.2336	2.0341	4.9804	3.18E-07	3.66E-05
	Morgenstern-Price	FS_{min}	7.0000	25.0000	25.9608	1.9925	5.1988	1.00E-07	1.53E-05
		Pf_{max}	4.7500	26.0000	26.4172	2.0455	4.9738	3.29E-07	3.66E-05
		Rv_{max}	5.0000	25.7500	26.2336	2.0336	4.9768	3.24E-07	3.73E-05
2	Bishop	FS_{min}	7.7500	21.7500	24.8095	1.8132	4.3463	6.93E-06	1.54E-03
		Pf_{max}	6.5000	21.0000	23.6666	1.8349	4.2591	1.03E-05	1.92E-03
		Rv_{max}	6.7500	20.7500	23.5563	1.8273	4.2635	1.01E-05	1.95E-03
	Janbu	FS_{min}	7.2500	20.7500	23.7641	1.6624	3.4405	2.90E-04	6.04E-02
		Pf_{max}	7.0000	20.7500	23.6595	1.6680	3.4367	2.95E-04	5.91E-02
		Rv_{max}	7.2500	20.7500	23.7641	1.6624	3.4405	2.90E-04	6.04E-02
	Janbu (f_0)	FS_{min}	7.5000	21.2500	24.2867	1.8049	4.1725	1.51E-05	3.25E-03
		Pf_{max}	6.7500	20.7500	23.5563	1.8191	4.1244	1.86E-05	3.60E-03
		Rv_{max}	7.0000	20.7500	23.6595	1.8119	4.1279	1.83E-05	3.68E-03
	Spencer	FS_{min}	7.7500	21.7500	24.8095	1.8116	4.3461	6.93E-06	1.54E-03
		Pf_{max}	6.2500	21.2500	23.7809	1.8415	4.2554	1.04E-05	1.88E-03
		Rv_{max}	6.7500	20.7500	23.5563	1.8253	4.2610	1.02E-05	1.97E-03
	Morgenstern-Price	FS_{min}	7.7500	21.7500	24.8095	1.8109	4.3447	6.98E-06	1.55E-03
		Pf_{max}	6.2500	21.2500	23.7809	1.8408	4.2542	1.05E-05	1.89E-03
		Rv_{max}	6.7500	20.7500	23.5563	1.8245	4.2597	1.02E-05	1.98E-03

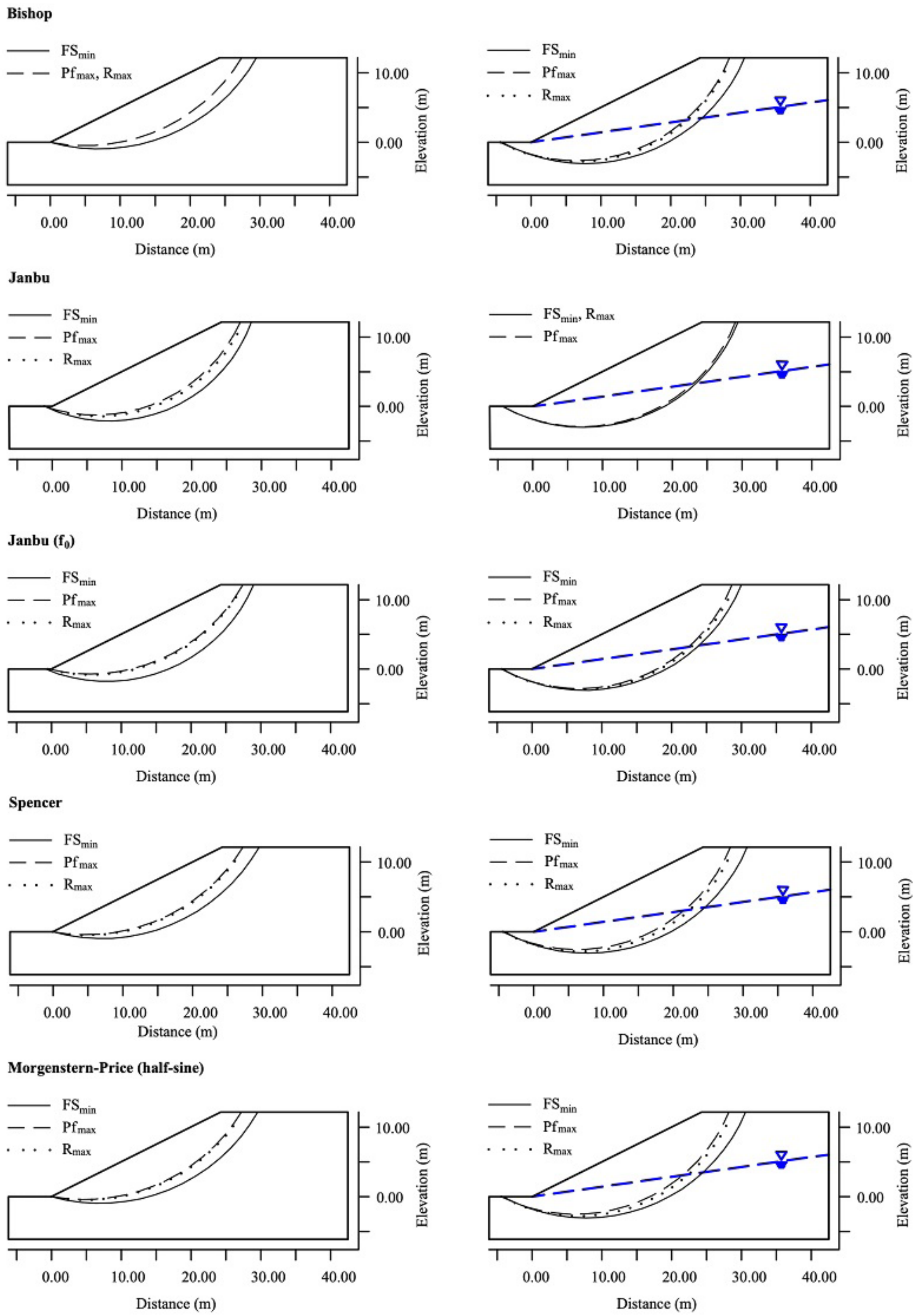

Figure 2. Deterministic and probabilistic critical slip surfaces.

Rv_{max} indentification criterion, because a Pf_{max} surface can be shallow enough to mobilize a volume corresponding to a relatively low failure consequence. On the other hand, there may be another surface with Pf slightly smaller than Pf_{max}, but which mobilizes a volume of soil capable of causing more severe consequences if it ruptures.

2.8 Cumulative distribution function

In an attempt to explain the variability of the probabilistic analysis responses regarding the found critical surfaces, the constant a was used to modify the limit state function. This modification enables the construction of a cumulative density function $F_X(\boldsymbol{X})$ of $FS(\boldsymbol{X})$, such that $F_X\left(\boldsymbol{X}\right) = P\left[FS\left(\boldsymbol{X}\right) \le a\right]$ with $a \in \left[0.5, 3.5\right]$, as shown in Figure 3:

Differences are observed in the probability curves due to the choice of the limit equilibrium methods, the different critical surfaces identified and the existence of acting or non-acting pore water pressure. In the presented analyses, the probability

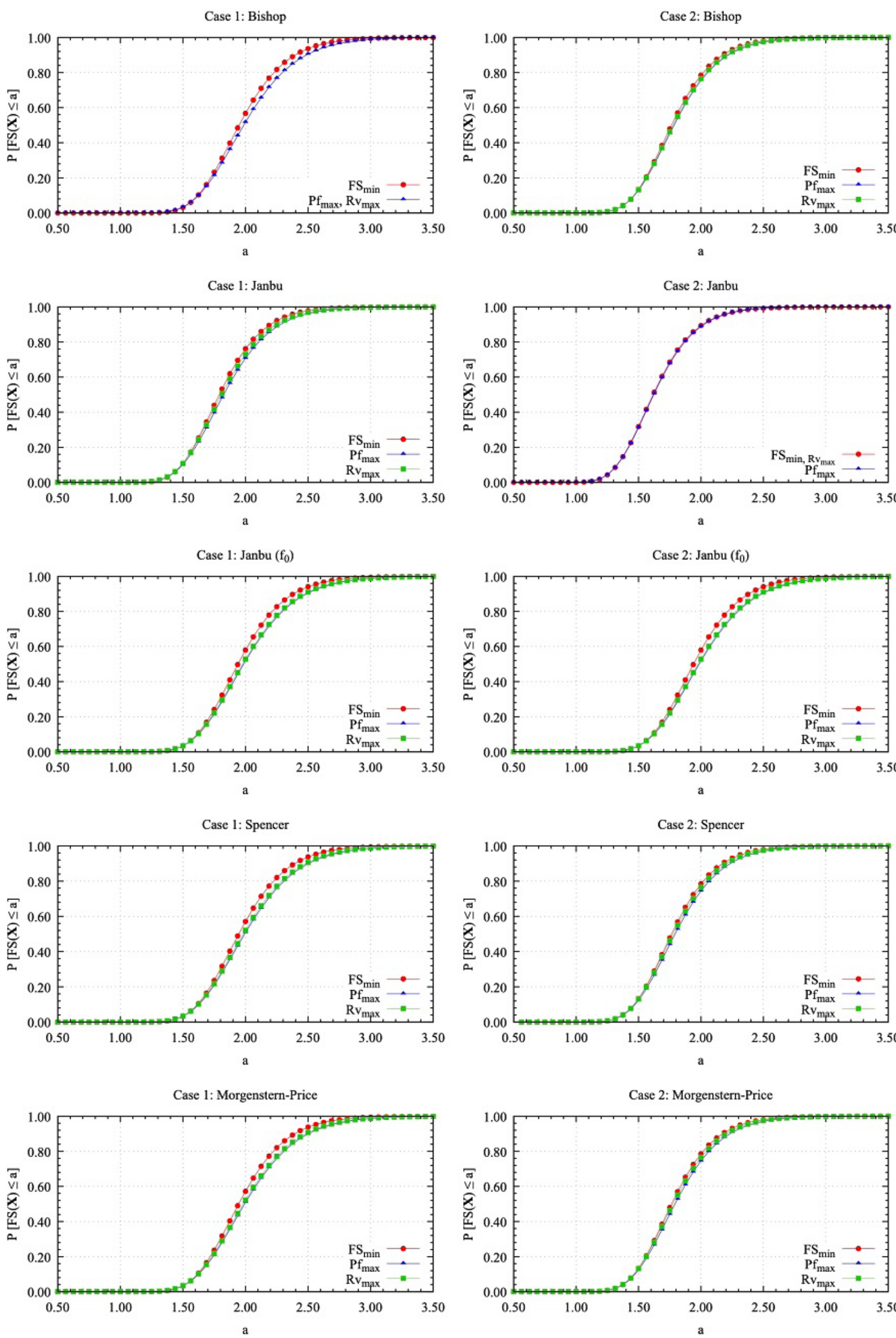

Figure 3. Cumulative density functions of critical slip surfaces.

curves of the FS_{min} surfaces were more distant from the curves of Pf_{max} and Rv_{max}. However, the curves of Pf_{max} and Rv_{max} were much closer to each other, when compared to those of FS_{min}.

2.9 Probability density function

The curve representing the probability density function $f_X(\boldsymbol{X})$ of $FS(\boldsymbol{X})$ can be constructed from the numerical derivation of $F_X(\boldsymbol{X})$, so that $F_X{}'(\boldsymbol{X}) = f_X(\boldsymbol{X})$. Figure 4 presents the curve $f_X(\boldsymbol{X})$ for the cases analysed:

The probability curves $f_X(\boldsymbol{X})$ facilitate the visualization of the variability of $FS(\boldsymbol{X})$, because the differences become more apparent regarding to those of $F_X(\boldsymbol{X})$ curves. No change in behaviour occurs in relation to the curves $F_X(\boldsymbol{X})$, because they are just different ways to show the same results.

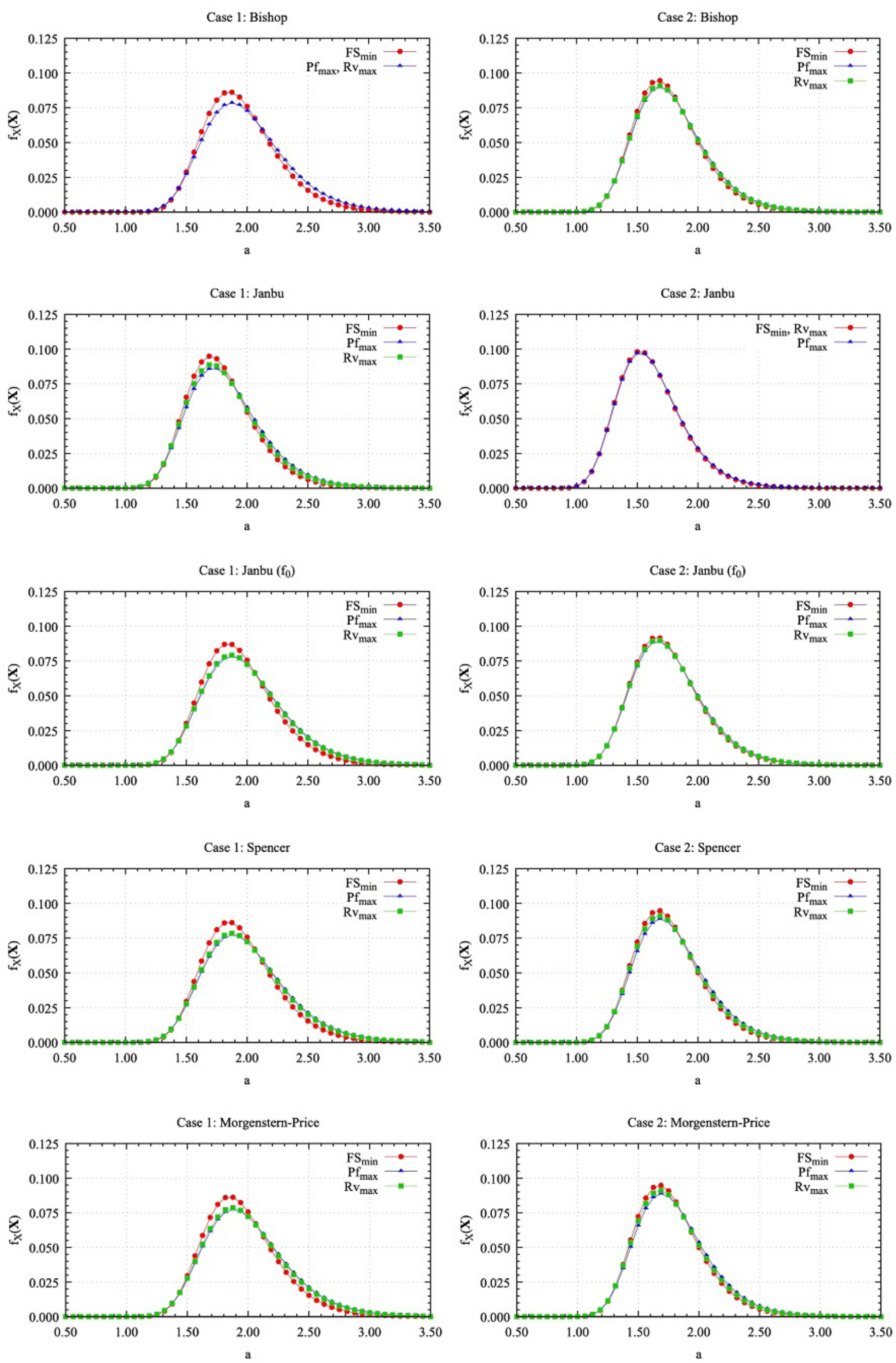

Figure 4. Probability density functions of critical slip surfaces.

2.10 Fixed slip surface

To complement the analyses already presented, the same procedure of construction of $F_X(\boldsymbol{X})$ and $f_X(\boldsymbol{X})$ was employed to a slip surface fixed in the region delimited by the set of all critical surfaces, according to Figure 5:

These analyses are intended to show the differences in the probability distributions of *FS(**X**)* of the same slip surface, resulting from the choice of different limit equilibrium methods in direct coupling. Figure 6 presents the probability distribution curves of *FS(**X**)* of all critical surfaces, including the surface fixed in the critical region:

It is observed that the various possibilities of direct coupling produce different probabilistic responses in at least two aspects. For the same sliding surface, the curves of probability distributions of *FS(**X**)* do not coincide with each other. Furthermore, when the analyses involve the investigation of critical surfaces, the results show that these surfaces may be non-coincident. The non-coincidence of the identified critical surfaces results in a set of deterministic and probabilistic surfaces that define a critical region in the analysed cross section instead of a single slip surface. These results explain the existence of variability in the responses provided by the most widespread methods of limit equilibrium in geotechnical practice. Larger differences are observed in the responses given by the uncorrected Janbu method. These differences evidence the fact that the correction proposed by the author of the method, through correction factor f_0, ensures a better approximation of its response regarding to the other methods. It is interesting to note that this procedure

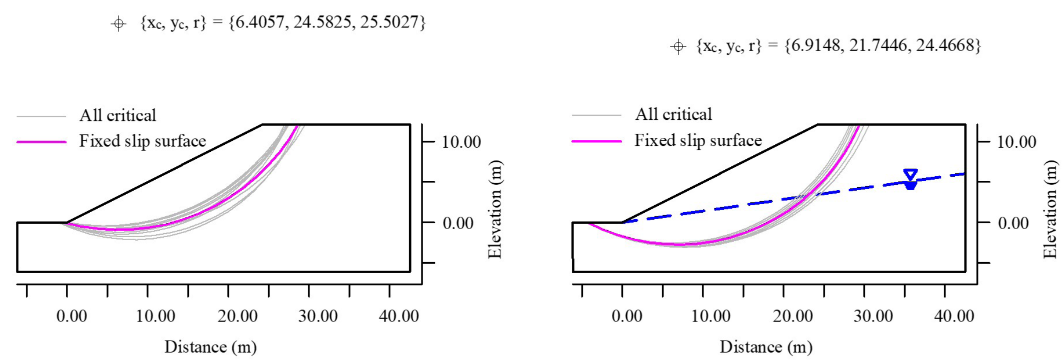

Figure 5. An overlap of all critical surfaces identified by deterministic and probabilistic criteria and different limit equilibrium methods employed in direct coupling.

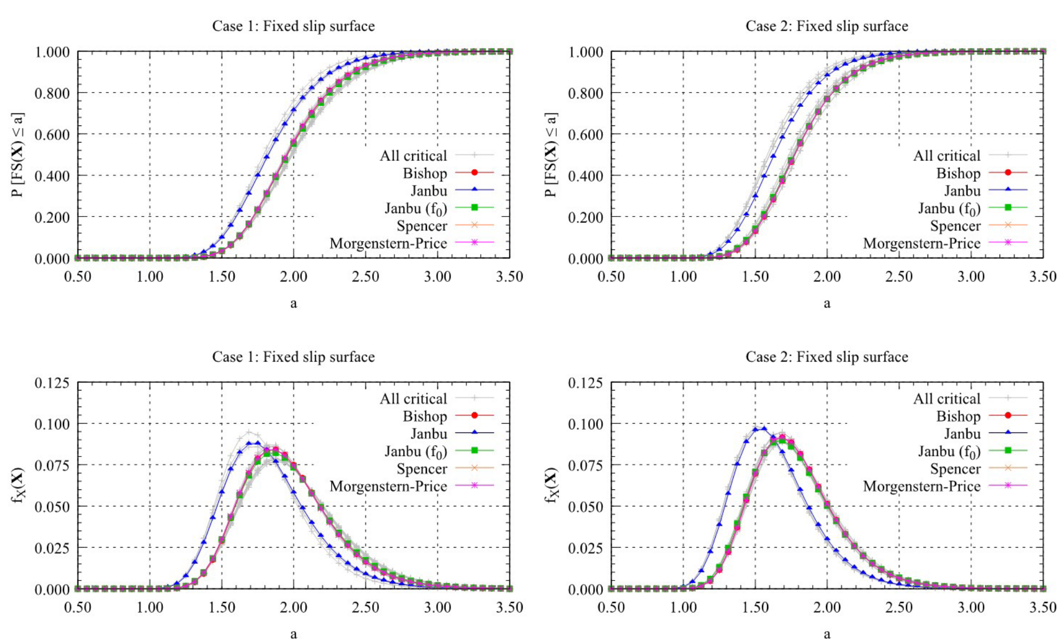

Figure 6. *FS(**X**)* probability distribution curves of the fixed slip surface and all critical surfaces.

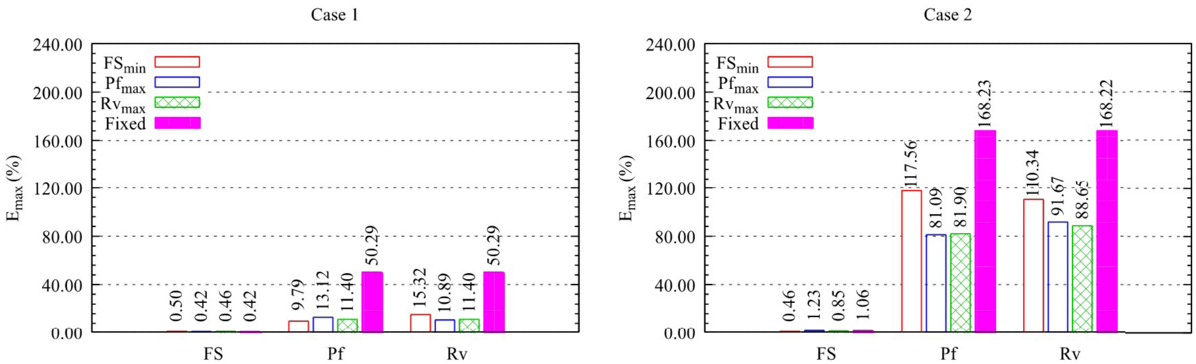

Figure 7. E_{max} of the answers provided by the limit equilibrium methods, relative to the fixed and critical surfaces.

provides, in addition to *Pf*, the probability that *FS(**X**)* assumes a value less than or equal to *a*, for any value of *a*. Thus, it is possible to calculate, for example, the probability of *FS(**X**)* violating values recommended by technical standards or any *a* value of interest.

Another way of showing the variability of the responses of the limit equilibrium methods is presented. From then on, responses from the uncorrected Janbu method were discarded, due to its high discrepancy when compared to the other methods. The *FS*, *Pf* and *Rv* values calculated by the different limit equilibrium methods were compared, restricting this comparison to the critical surfaces identified by the same criterion. All identified critical surfaces have a *FS*, *Pf* and *Rv* value, as shown in Table 4. Thus, the maximum relative error (E_{max}) refers to the results of surfaces belonging to the same set of critical surfaces, identified by the criteria FS_{min}, Pf_{max} or Rv_{max}. The fixed slip surface results are also presented. Figure 7 shows the E_{max} values for the analyzed cases:

In both cases analysed, E_{max} values of *FS* were relatively low, between 0.42% and 1.23%. E_{max} values are quite pronounced in the probabilistic responses, especially for case 2, in which the pore water pressure acts on the slope. The highest E_{max} values of *Pf* and *Rv* refer to the fixed slip surface, reaching 50.29% for case 1 and 168.22% for case 2. However, it was observed that E_{max} decreased when the responses of different surfaces, defined by the same identification criteria, were compared, between 9.79% and 15.32% in case 1, and between 81.09% and 117.56% in case 2. These results suggest that the consideration of a set of critical surfaces, according to the identification criteria presented, tends to minimize the variability of the probabilistic responses provided by different limit equilibrium methods directly coupled to FORM. On the other hand, if only one slip surface is considered, even if positioned in the critical region of the slope, the variability of the probabilistic responses increases significantly as a function of the choice of method, while the deterministic responses are practically identical.

3. Concluding remarks

In this paper, analyses of slope stability were presented referring to two cases of a slope collected in the literature. Both cases served as benchmarks for validating the Morgenstern-Price method implemented in RASS. The deterministic responses of *FS* and λ were presented, providing relative errors of less than 0.3%. Next, the scheme of methods used in the direct coupling of limit equilibrium methods to the FORM was presented, which made it possible to calculate the probabilities of shear failure of the slope, considering *c'* and ϕ' as random variables of the problem. Five limit equilibrium methods and three critical surface identification criteria were employed, based on FS_{min}, Pf_{max} e Rv_{max}, which allowed the identification of a critical fault region in the slope cross section instead of a single surface. In addition, the results showed the importance of identifying critical surfaces using probabilistic and not just deterministic criteria, in order to prevent probability calculations from being performed only for surfaces determined by FS_{min}.

The deterministic and probabilistic results showed that the uncorrected Janbu method provides very conservative responses regarding to the other tested methods, reinforcing the importance of adopting the f_0 correction factor proposed by the author of the method. Another important conclusion is that for the analyzed cases, the critical surfaces defined by FS_{min} showed very low variability in the *FS* responses due to the choice of limit equilibrium method. The greatest variability observed refers to the probabilistic responses of the same surface, fixed in the critical region of the slope. On the other hand, less variability was observed in the surfaces identified by the probabilistic criteria, being lower in case 1 than in case 2.

The use of the analysis framework presented in this work, in which the slope stability analyses are carried out jointly by different limit equilibrium methods and according to deterministic and probabilistic approaches, enriches the range of information available to the analyst, assisting in the engineering decision making process and in the geotechnical risk management. As there is no method that provides a real answer to the problem, because all methods adopt simplifying assumptions to make the problem statically determined, one cannot claim categorically which limit equilibrium method is better than the others. Thus, the authors suggest the use of more than one limit equilibrium method and also the adoption of deterministic probabilistic criteria to identify critical surfaces, because in general these surfaces are not coincident.

Acknowledgements

The authors gratefully acknowledge the financial support of the Coordenação de Aperfeiçoamento de Pessoal de Nível Superior - Brasil (CAPES) - Finance Code 001.

Declaration of interest

The authors have no conflicts of interest to declare. All co-authors have observed and affirmed the contents of the paper and there is no financial interest to report.

Authors' contributions

Higor Biondo de Assis: Conceptualization, Data curation, Methodology, Software, Writing – original draft. Caio Gorla Nogueira: Conceptualization, Methodology, Supervision, Validation, Writing – review & editing.

Data availability

The datasets generated analyzed in the course of the current study are available from the corresponding author upon request.

List of symbols

a	Constant used in the modification of the limit state function for the construction of the curves $F_X(\boldsymbol{X})$ and $f_X(\boldsymbol{X})$
b_i	Width of *i*th slice
c'	Effective soil cohesion
c_i'	Effective soil cohesion along the base of the *i*th slice
C	Constant representing the consequence associated to the slope failure
$f(x)$	Interslice force function
	Interslice force function value on the left side of *i*th slice
f_{i-1}	Interslice force function value on the right side of *i*th slice
h_i	Height of *i*th slice
i	Integer counter for the number of slices
j	Integer counter that depends on i
n	Total amount of slices
r	Radius of the circle describing the critical slip surface
x_c	Abscissa of the centre of the circle describing the critical slip surface
x_L	Abscissa of the left end of the slip surface
x_R	Abscissa of the right end of the slip surface
y_c	Ordinate of the centre of the circle describing the critical slip surface
$\boldsymbol{y}^*$	Design point
COV_X	Coefficient of variation of the random variable X
E	Normal interslice force
E_i	Normal interslice force acting on the left side of the *i*th slice
E_{i-1}	Normal interslice force acting on the right side of the *i*th slice
E_{max}	Maximum relative error
FS	Factor of safety
FS_{min}	Minimum factor of safety
$FS(\boldsymbol{X})$	Factor of safety as a function of the random variable vector
$F_X(\boldsymbol{X})$	Cumulative density function of $FS(\boldsymbol{X})$
$f_X(\boldsymbol{X})$	Probability density function of $FS(\boldsymbol{X})$
$g(\boldsymbol{X})$	Limit state function
$P[\bullet]$	Probability of occurrence of the condition of interest $[\bullet]$
Pf	Probability of failure
Pf_{max}	Maximum probability of failure
PDF_X	Probability density function of the random variable X
Q_i	External force acting on the *i*th slice
R_i	Sum of the shear resistances contributed by all the forces acting on the *i*th slice except the normal shear interslice forces
R_n	Sum of the shear resistances contributed by all the forces acting on the *n*th slice except the normal shear interslice forces
Rv	Risk value given by the constant representing the volume of soil mobilised at the slope failure
Rv_{max}	Maximum risk value
S	Tangential interslice force
T_i	Sum of the components of the R_i forces relating to the *i*th slice that tend to cause instability
T_n	Sum of the components of the R_n forces relating to the *n*th slice that tend to cause instability
U_i	Resultant water force acting on the base of the *i*th slice
W_i	Self-weight of *i*th slice
$\boldsymbol{X}$	Random variable vector x Abscissa of slope cross section
α_i	Angle formed between the horizontal and base of the *i*th slice
β	Reliability index
γ	Soil unit weight
λ	Scaling factor
μ	Non-negative exponent specified in function $f(x)$
μ_X	Mean value of the random variable X
ν	Non-negative exponent specified in function $f(x)$
$\Phi(\bullet)$	Standard normal cumulative distribution function

ϕ' Effective friction angle of the soil

Φ_i Variable used to rearrange the equations of the Morgenstern-Price method

φ_i' Effective soil friction angle along the base of the ith slice

Φ_{i-1} Variable used to rearrange the equations of the Morgenstern-Price method

Ψ_{i-1} Variable used to rearrange the equations of the Morgenstern-Price method

Ψ_j Variable used to rearrange the equations of the Morgenstern-Price method

ω_i Angle between the vertical and the direction of the external force Q_i acting on the ith slice

$\mathbb{X}$ Physical space of random variables

$\mathbb{Y}$ Standard Gaussian space

References

Abramson, L.W., Lee, T.S., Sharma, S., & Boyce, G.M. (2001). *Slope stability and stabilization methods.* John Wiley & Sons.

Ang, A.H., & Tang, W.H. (1984). *Probability concepts in engineering planning and design: decision, risk, and reliability* (Vol. 2). John Wiley & Sons.

Bishop, A.W. (1955). The use of the slip circle in the stability analysis of slopes. *Geotechnique*, 5(1), 7-17.

Cho, S.E. (2007). Effects of spatial variability of soil properties on slope stability. *Engineering Geology*, 92(3–4), 97-109. http://dx.doi.org/10.1016/j.enggeo.2007.03.006.

Cho, S.E. (2010). Probabilistic assessment of slope stability that considers the spatial variability of soil properties. *Journal of Geotechnical and Geoenvironmental Engineering*, 136(7), 975-984. http://dx.doi.org/10.1061/(ASCE)GT.1943-5606.0000309.

Fenton, G.A., & Griffiths, V.D. (2008). *Risk assessment in geotechnical engineering*. John Wiley & Sons New Jersey.

Fredlund, D.G., & Krahn, J. (1977). Comparison of slope stability methods of analysis. *Canadian Geotechnical Journal*, 14(3), 429-439.

Hasofer, A.M., & Lind, N.C. (1974). Exact and invariant second-moment code format. *Journal of the Engineering Mechanics Division*, 100(1), 111-121.

Husein Malkawi, A.I., Hassan, W.F., & Abdulla, F.A. (2000). Uncertainty and reliability analysis applied to slope stability. *Structural Safety*, 22(2), 161-187. http://dx.doi.org/10.1016/S0167-4730(00)00006-0.

Janbu, N. (1954a). Application of composite slip surface for stability analysis. In *Proceedings of European Conference on Stability of Earth Slopes* (pp. 43-49), Sweden, 1954.

Janbu, N. (1954b). *Stability analysis for slopes with dimensionless parameters* [Doctoral thesis]. Harvard University Soil Mechanics Series.

Janbu, N. (1973). Slope stability computations. In R.C. Hirschfeld and S.J. Poulos (Eds.), *Embankment-dam engineering*. John Wiley & Sons.

Ji, J., Zhang, C., Gao, Y., & Kodikara, J. (2018). Effect of 2D spatial variability on slope reliability: a simplified FORM analysis. *Geoscience Frontiers*, 9(6), 1631-1638. http://dx.doi.org/10.1016/j.gsf.2017.08.004.

Jiang, S., Huang, J., Griffiths, D.V., & Deng, Z. (2022). Advances in reliability and risk analyses of slopes in spatially variable soils: a state-of-the-art review. *Computers and Geotechnics*, 141, 104498. http://dx.doi.org/10.1016/j.compgeo.2021.104498.

Lebrun, R., & Dutfoy, A. (2009). Do Rosenblatt and Nataf isoprobabilistic transformations really differ? *Probabilistic Engineering Mechanics*, 24(4), 577-584. http://dx.doi.org/10.1016/j.probengmech.2009.04.006.

Leonel, E.D., Beck, A.T., & Venturini, W.S. (2011). On the performance of response surface and direct coupling approaches in solution of random crack propagation problems. *Structural Safety*, 33(4), 261-274. http://dx.doi.org/10.1016/j.strusafe.2011.04.001.

Melchers, R.E., & Beck, A.T. (2018). *Structural reliability analysis and prediction*. John Wiley & Sons.

Morgenstern, N.R., & Price, V.E. (1965). The analysis of the stability of general slip surfaces. *Geotechnique*, 15(1), 79-93.

Phoon, K. (2008). *Reliability-based design in geotechnical engineering: computations and applications*. CRC Press.

Phoon, K., & Kulhawy, F.H. (1999). Characterization of geotechnical variability. *Canadian Geotechnical Journal*, 36(4), 612-624.

Rackwitz, R., & Fiessler, B. (1978). Structural reliability under combined random load sequences. *Computers & Structures*, 9(5), 489-494. http://dx.doi.org/10.1016/0045-7949(78)90046-9.

Siacara, A.T., Beck, A.T., & Futai, M.M. (2020). Reliability analysis of rapid drawdown of an earth dam using direct coupling. *Computers and Geotechnics*, 118, 103336. http://dx.doi.org/10.1016/j.compgeo.2019.103336.

Siacara, A.T., Napa-García, G.F., Beck, A.T., & Futai, M.M. (2022). Reliability analysis of an earth dam in operating conditions using direct coupling. *SN Applied Sciences*, 4(4), 99. http://dx.doi.org/10.1007/s42452-022-04980-7.

Spencer, E. (1967). A method of analysis of the stability of embankments assuming parallel inter-slice forces. *Geotechnique*, 17(1), 11-26.

Spencer, E. (1973). Thrust line criterion in embankment stability analysis. *Geotechnique*, 23(1), 85-100.

Zhang, J., & Huang, H.W. (2016). Risk assessment of slope failure considering multiple slip surfaces. *Computers and Geotechnics*, 74, 188-195. http://dx.doi.org/10.1016/j.compgeo.2016.01.011.

Zhu, D., Lee, C., Qian, Q., & Chen, G. (2005). A concise algorithm for computing the factor of safety using the Morgenstern Price method. *Canadian Geotechnical Journal*, 42(1), 272-278.